Bull. Chem. Soc. Jpn., 70, 2341—2356 (1997)

Accounts

Zeolitic Membranes: Synthesis, Properties, and Prospects

Masahiko Matsukata* **and Eiichi Kikuchi†**

Department of Chemical Engineering, Osaka University, 1-3 Machikaneyama, Toyonaka, Osaka 560

†School of Science and Engineering, Waseda University, 3-4-1 Okubo, Shinjyuku-ku, Tokyo 169

(Received January 7, 1997)

This article is intended to describe recent progress in the synthesis of zeolitic membranes and their permeation properties. While hydrothermal synthesis has been widely employed for zeolitic-membrane synthesis, the development of a new technique for zeolite synthesis, vapor-phase transport (VPT), has enabled us to prepare pinhole-free, zeolite-porous support composite membranes. This article consists of three sections that describe: a survey of the hydrothermal synthesis of zeolitic membranes, our synthesis results and the formation mechanism of zeolitic membranes by the VPT method as well as some permeation results to show the prospects of zeolitic membranes.

Inorganic membranes were the first membranes which found practical application in large-scale gas-separation processes in the 1940's. An alumina membrane was used to separate isotopes of uranium based on the difference in the molecular weights of their hexafluorides. New sophisticated techniques of thin polymeric membrane preparation, gas-separation processes using polymeric membranes, were commercialized. Polymeric membranes had both high permselectivity and rapid permeation. For several decades, the research and development efforts in membrane processes were directed to polymeric membranes, while inorganic membranes were largely forgotten. Due to their instability in organic solvents and at high temperatures, however, practical applications of polymeric membranes have been limited to these processes operating at slightly above room temperature.

There is strong interest in membranes made of inorganic materials, such as ceramics and metals for applications in separation processes, owing to their superior characteristics of thermal, mechanical and structural stabilities, and of chemical resistance. In order to develop a new generation of high-temperature resistant membranes, researchers have turned back to the development of inorganic membranes.

Inorganic membranes can be classified into two types, nonporous (dense) and porous membranes. The first well-studied inorganic membranes were dense palladium[1] and its alloys,[2] which are permeable only to hydrogen. Following palladium-based membranes, other types of dense inorganic membranes permselective to oxygen, for instance, silver and stabilized zirconia, have been developed.[3] The types of permselective dense membranes, however, are limited to motivate the development of porous inorganic membranes.

Based on the definition by the International Union of Pure and Applied Chemistry (IUPAC), porous materials, such as adsorbents and porous membranes, are classified in relation to their pore size, as follows:

1. Pores with widths exceeding about 50 nm are called *macropores*;
2. Pores with widths between 2 and 50 nm are called *mesopores*; and
3. Pores with widths not exceeding about 2 nm are called *micropores*.

The membranes used in the practical applications today are mostly macroporous with pore diameters of 0.1—100 μm. They include alumina, zirconia, and porous glass membranes. Porous metal membranes are available, though they are relatively limited in the extent of industrial use because of their costs.

The transport of gases in macropores is governed by the viscosity of the gas (Poiseuille flow), Knudsen diffusion, or flow in the transition between them. Membranes with macropores are, thus, not expected to show sufficient selectivities for gas separation, although they show high permeability. In smaller pores, mesopores, surface diffusion and capillary condensation phenomena can play an important role in the transport of molecules in addition to Knudsen diffusion. Mesoporous membranes, including γ-alumina, titania and zirconia, with an average pore diameters of 2—10 nm have been prepared by sol–gel techniques. When the pore size is comparable to the molecular dimensions, a molecular sieving property appears, thereby leading to large selectivity.

Therefore, the current research is mainly focusing on the development of microporous membranes.

The first study that attracted attention to microporous membranes was on a silica membrane, reported by Gavalas et al., who prepared a SiO_2 layer within the pores of a Vycor glass tube by SiH_4 oxidation.[4—6] This SiO_2 membrane was highly selective to H_2 permeation with a permselectivity of H_2/N_2 = ca. 3000 at 723 K. Following this study, they succeeded to prepare of H_2-permselective SiO_2, TiO_2, Al_2O_3, B_2O_3 membranes by chemical-vapor deposition using their chloride precursors within the pores of a Vycor glass tube. These membranes show permselectivities of H_2/N_2 = 1000—5000 at 723 K. Another noteworthy H_2-permselective membrane was a SiO_2 membrane, which was prepared on an alumina support with an average pore diameter of 1 μm by a sol–gel method.[7] Its permselectivity of H_2/N_2 was about 400. Microporous glass membranes with the pore width of $0.5 < d < 2.0$ nm were prepared by attenuation from glass melts.[8,9] The permselectivities of H_2/N_2 and He/CH_4 at 303 K were 235 and 11700, respectively. Another method for preparing microporous membranes has been to use carbon of which membranes are obtained by carbonization of polymeric precursors.[10,11]

Besides the amorphous materials mentioned above, microporous crystals have been of interest as membrane materials in recent years because they have extremely narrow pore-size distributions, which is not the case for amorphous materials.

Zeolites, a class of microporous crystalline aluminosilicate materials, have been extensively studied and utilized in chemical and physical processes, such as in gas separation and heterogeneous catalysis. Adsorptive separation processes with granular molecular sieves are operated in a batchwise manner. If membranes could be composed of a sort of zeolites, it would be possible to carry out separation continuously without any changes in the phase, and to substitute these processes with the membrane separation ones.

Apart from their high thermal resistance, high mechanical strength and chemical inertness, zeolites have the following advantageous features when used as a membrane.

1. Micropore systems of zeolites are inherent for the structure. Pore diameters in zeolites are determined by the aperture with 4, 6, 8, 10 or 12-membered rings of oxygen anions. The maximum values of the pore opening were calculated to be 0.26, 0.34, 0.42, 0.63, and 0.74 nm, respectively.

2. Inner surface of zeolites can be readily modified. Both the actual pore size and the affinity between adsorbed molecules and the pore-wall depend on the type of cation, and are precisely controllable by ion-exchange. The outer surface can also be selectively modified by chemical-vapor deposition.[12]

3. The hydrophilic/hydrophobic nature of zeolites can be tuned by changing the SiO_2/Al_2O_3 ratio in the framework of zeolites. The cation that balances the negative charge associated with the framework aluminum ions causes an electrostatic field in zeolites. Thus, the pores of aluminum-rich zeolites are occupied by water molecules, while a decrease in the aluminum content leads to the hydrophobic nature.

4. Since zeolites exhibit catalytic properties, they can be applied to catalytic membrane reactors. A few concepts of membrane reactors using zeolitic membranes have been proposed.[13,14]

Due to the reasons described above, increasing attention has been paid to the preparation of zeolitic membranes. Whereas zeolitic membranes were first proposed in the 1980's,[15—18] studies of them started to be reported in scientific journals in the early 1990's. In this account, previous reports on the preparation of zeolitic membranes will be reviewed first. We have proposed a new synthetic method, a dry-gel conversion technique to prepare zeolitic membranes via vapor-phase transport. Recent progress of our studies concerning the preparation of zeolitic membranes and their properties will be summarized.

Hydrothermal Synthesis of Zeolitic Membranes

Zeolitic membranes have typically been prepared from hydrogels or sols composed of SiO_2, Al_2O_3, Na_2O, H_2O, and organic templating agents. More or less, most of the studies have employed a conventional hydrothermal synthe-

Table 1. Self-Supporting MFI Membranes

	Silica source	Alumina source	Gel composition ($Na_2O : SiO_2 : Al_2O_3$: TPA : H_2O)	Substrate	Crystallization	Thickness μm
Sano et al.[19]	CS	$Al(NO_3)_3$	0.05 : 1 : 0.01 : 0.1 : 40—100	Teflon®	373—473 K 2—17 d	30—100
Sano et al.[20,21]	CS	$Al(NO_3)_3$	0.05 : 1 : 0.01 : 0.1 : 80	Teflon®	443 K 2 d	30—100
Tsikoyiannis and Haag[22]	CS	—	2.2 : 100 : 0 : 5.22 : 2832	Teflon® Silver Stainless steel Vycor® disk	453 K 0.3—9 d	20—250
Sano et al.[23]	CS	$Al(NO_3)_3$	0.05 : 1 : 0—0.01 : 0.1 : 80	Cellulose	443 K 2 d	500
Kiyozumi et al.[24]	CS	$Al(NO_3)_3$	0.01 : 0.05—0.1 : 1 : 0—0.02 : 20—400	Mercury	393—453 K 2 d	

CS: colloidal silica.

Table 2. Supported-MFI Membranes

	Si source	Al source	Gel composition ($Na_2O : SiO_2 : Al_2O_3 : TPA : H_2O$)	Support (pore diameter)	Crystallization	Thickness μm
Geus et al.[25]	Aerosil 200	—	1.6 : 1 : 0 : 1.5 : 166.66	Clay, zirconia	453 K, 1—5 d	100
Geus et al.[26]	Aerosil 200, CS	—	— : 100 : 0 : 6 : 6330	Sintered metal (10 μm), Stainless steel	453 K, 1—7 d	60—400
Jia et al.[27]	Aerosil 130	—	0.75 : 9 : 0 : 1.0 : 70	Ceramic disk	453 K, 3—72 h	5
Sano et al.[28]	CS	—	0.05 : 1 : 0 : 0.1 : 80	Stainless steel (0.5—2 μm)	443 K, 2 d	400—500
Masuda et al.[29]	SS	$Al_2(SO_4)_3$	34 : 71 : 1 : —	α-Alumina (2 μm)	473 K, 2 d	10—25
Jia et al.[30]	Aerosil 130	—		γ-Alumina (5 nm)	453 K, 3—72 h	10
Meriaudeau et al.[31]	TEOS	—	— : 1 : 0 : 0.051 : 22.5	Porous glass (10—20 μm)	448 K, 72 h	150
Bai et al.[32]	Aerosol	—	0.071 : 1 : 0 : 0.071 : 42	γ-Alumina (5 nm)	453 K, 12 h	10
Yan et al.[33]	CS	—	2 : 6 : 0.005 : 1 : 571 : 1	α-Alumina (0.5 μm)	448 K, 16 h	10
Yan et al.[34]	TEOS	Al foil	0—4 : 6 : 0—0.06 : 1 : 96—700	α-Alumina (0.5 μm)	448 K, 4—24 h	10
Vroon et al.[35]	Silica	—	5.3 : 100 : 0 : 30 : 1420	α-Alumina	393 K, 3 d	5
Chiou et al.[36]	TEOS	—	5 : 100 : 0 : 10 : 10000	Anodic alumina (0.2 μm)	473 K, 1—4 d	130
Kusakabe et al.[37]	Aerosil 200	—	— : 1 : 0 : 1.0 : 100	γ-Alumina (5—10 nm) α-Alumina (0.95, 0.15 μm)	448 K, 12—24 h	20 —30

TPA: tetrapropylammonium ion, IPA: isopropylalcohol, TEOS: tetraethylorthosilicate, CS: colloidal silica, SS: sodium silicate solution.

Table 3. Supported-Zeolitic Membranes Other than MFI

	Products	Si	Al	Composition ($Na_2O : SiO_2 : Al_2O_3 : TPA : H_2O$)	Crystallization	Support	Thickness μm
Suzuki et al.[38]	MOR	CS	$Al_2(SO_4)_3$	0.38 : 1 : 0.025 : 0 : 40	433 K 40 h	Silica–alumina, Quartz glass	23
Geus et al.[25]	ANA	Aerosil 200	—	1.6 : 1 : 0 : 1.5 : 166.66	453 K 1—5 d	α-Alumina	
Masuda et al.[39]	LTA	Na_2SiO_3	$Al(OH)_3$	—	343—373 K 6—18 h	α-Alumina	5—25
Mimura et al.[40]	ANA	CS	PNC	67.5 : 67.3 : 1.0 : 1.0 : 3375	423—453 K 0.1—3 d	α-Alumina	60
Kita et al.[41]	LTA	SS	$Al(OH)_3$	2 : 2 : 1 : 0 : 120	373 K 3.5 h	α-Alumina	30
Yamazaki and Tsutsumi[42]	LTA	SS	$Al_2(SO_4)_3$	4.25 : 2.5 : 1.0 : 0 : 111	433 K 40 h	Silica	
Yamazaki and Tsutsumi[43]	MOR	CS	$NaAlO_2$	3 : 20 : 1 : 0 : 200	453 K 1—5 d	Stainless-steel filter	

PNC: Powdered natural clinoptilolite.

sis to produce a zeolitic thin layer. Typical silica sources for synthesizing MFI (particularly known as ZSM-5 zeolite) membranes are colloidal silica and silica powder (Aerosil). The tetrapropylammonium (TPA) cation has mainly been used as a templating agent.

Self-supporting zeolitic membranes can be synthesized on various substrates. Table 1 summarizes studies concerning the preparation of self-supporting zeolitic membranes. Sano and coworkers[19—21] first synthesized self-supporting MFI membranes on a Teflon® sleeve using a clear aqueous solution with a composition of 0.1 TPABr : 0.05 Na_2O : 0.01 Al_2O_3 : SiO_2 : 40—100 H_2O. Synthesis mixtures with H_2O/SiO_2 ratios > 70 were crystallized to form MFI membranes without stirring. Tsikoyiannis and Haag hydrothermally synthesized MFI layers with 20—250 μm thickness on various non-porous supports, such as a Teflon® slab.[22]

The mechanical strength of self-supporting zeolitic membranes is insufficient for their application in separation processes. Most of the studies on the synthesis of zeolitic membranes have been directed for use on porous supports.

High-silica MFI membranes have mainly been studied as summarized in Table 2. Supported MFI membranes have typically been prepared from hydrogels or sols composed of SiO_2, Al_2O_3, Na_2O, and TPA cation, similarly to the preparation of self-supporting membranes. A reactant mixture, in which a porous support is immersed, is placed in an autoclave. Typical MFI membranes have been synthesized on macroporous supports with a pore size of 0.1—10 μm, such as α-alumina and sintered stainless steel. A support with γ-alumina top layer with an average pore size of 5 nm was also used by Jia et al.[30] Table 3 summarizes the studies concerning other kinds of zeolitic membranes. The preparation of zeolite A (LTA)[29,41,42] and mordenite (MOR)[38,43] membranes have been extensively investigated.

Myatt et al.[44] claimed four possibilities for the formation of zeolitic membranes, as depicted in Fig. 1a: 1) The production of nuclei and the growth of crystals in the bulk solution, followed by their attraction to, or collision and association with, a substrate; 2) the production of nuclei in bulk solution, but diffusion to, and accumulation at, the support before significant growth has occurred; 3) the diffusion of colloidal amorphous aluminosilicate to, and concentration at, the substrate, providing more favorable conditions of nucleation and growth in the vicinity of the substrate; and 4) production of nuclei on the substrate surface, followed by growth. Figure 1b shows the mechanism proposed by Sano et al.,[21] who claimed that an MFI membrane forms through a successive accumulation of large MFI crystals of 5 to 10 μm and filling of voids among the large crystals with microcrystals. This corresponds to the first case of Myatt's mechanism. Valtchev et al.[46] studied the growth of MFI and FAU (Y type) zeolites on a copper substrate, and reported that there were three stages of film growth: 1) initial nucleation on the substrate, 2) a linear increase in crystal size, and 3) saturation of film growth, which is similar to the fourth mechanism proposed by Myatt et al. On the other hand, Kita et al.[41] suggested that a gel layer was first formed on the surface of a support, and then the gel layer was crystallized to LTA, being similar to the third mechanism. The MFI crystals prepared by Jansen et al.[45] were preferentially oriented parallel to the *b*-direction, and, thus, the straight channels of the pore system were perpendicular to the support surface. According to an in situ observation of crystallization, they proposed a formation mechanisms of such a preferentially oriented zeolite layer, as shown in Fig. 1c. First, large gel spheres containing no TPA were formed in the liquid phase, and the crystallization started at the interface of the gel spheres and the liquid

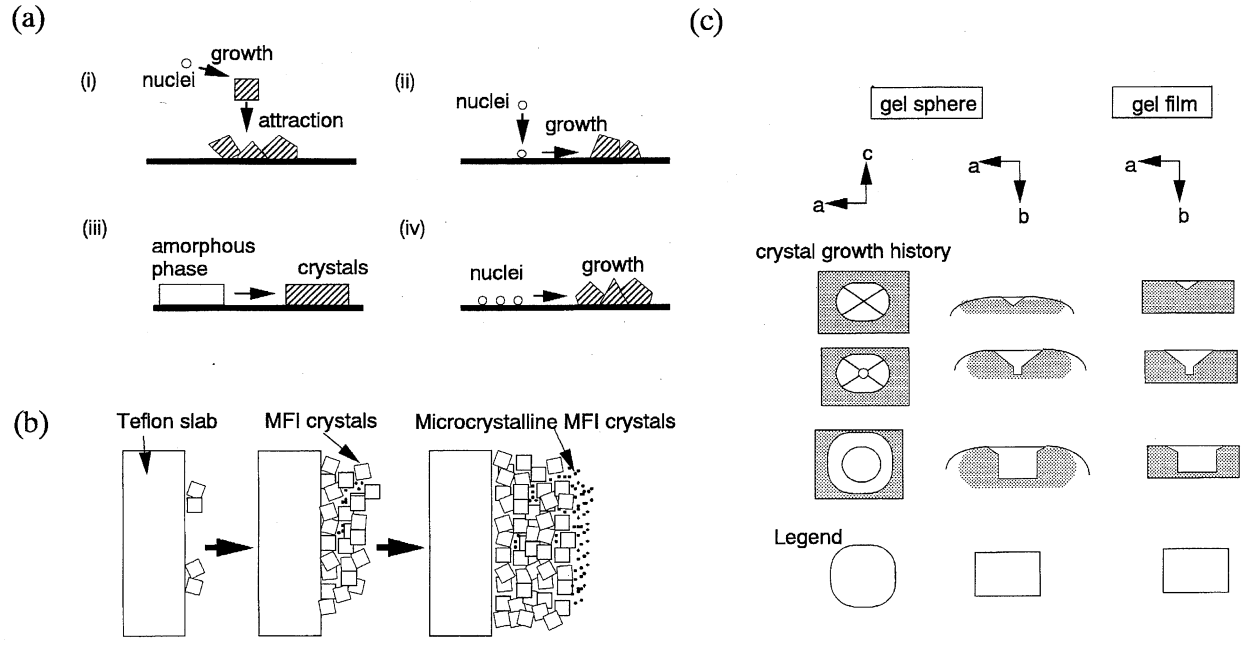

Fig. 1. Proposed growth mechanisms of zeolitic membranes. a) Sano et al.,[21] b) Myatt et al.,[44] and c) Jansen et al.[45]

phase. As soon as the gel spheres on which MFI crystals was formed attached the support surface, the support surface was attracted to the *ac*-plane, the largest plane of the crystal. As a result, the crystals were laterally oriented to the support surface. This is also similar to the third mechanism proposed by Myatt et al.

The intergrowth of zeolite crystals has often been observed,[22,27,33] and Yan et al.[33] have claimed that the intergrowth of zeolite crystals to fill the voids among crystals is cruicial for the synthesis of a compact zeolitic membrane under hydrothermal conditions.

The controlling factors for synthesizing a compact zeolitic layer have not yet been elucidated. However, a partial dissolution of the support during crystallization was often reported. Alumina[25,28,36] and glass[42] are easily leached during synthesis, and the dissolved Si^{4+} and Al^{3+} ions are expected to encourage nucleation and crystallization of zeolites on the support surface, leading to the formation of a continuos layer of zeolites. Additionally, the incorporation of dissolved Si or Al atoms into the framework of the resultant zeolite should greatly affect the types of zeolites formed.

Under these hydrothermal syntheses, the way to place the supports seems to affect the formation process of the zeolitic membranes, because nuclei or crystals homogeneously formed in the solution could deposit on the support by convection or diffusion.

Typically, porous supports were horizontally placed on the bottom of a Teflon® vessel.[28,40] On the other hand, Jansen et al.[45] adopted a vertical placement of the support. The support was positioned in the upper part of the synthesis mixture with the help of a Teflon® holder.

To form zeolite crystals only on the inner wall of a tube with γ-alumina top layer, Jia et al.[30] transferred a gel into the alumina tube, and plugged both ends with Teflon® caps. The tube was then placed in a Teflon®-lined autoclave. Yan et al.[33,34] placed a porous plate in an autoclave horizontally using a Teflon® holder. The upper level of the synthesis solution was, however, kept to dip only the bottom side of the support in the solution in order to grow zeolite crystals on the bottom side of the support.

A more sophisticated synthesis method has very recently been developed by Tsapatsis et al.,[47] who demonstrated that stable, colloidal suspensions of nano-sized zeolite L (LTL) particles can be formed from a clear solution, and then used for thin-film preparation. The average size of zeolite particles in the suspension was as small as 20 nm. A thin layer consisting of nano-LTL particles can be grown in an aluminosilicate sol. This was the first successful case to separate the nucleation process from the growth of zeolites during membrane synthesis in the hydrothermal method.

Synthesis of Zeolitic Membranes by Solid Dry-Gel Conversion via Vapor-Phase Transport

Bibby and Dale[48] first synthesized a zeolite from a non-aqueous system, suggesting that water is not essential as a solvent for the crystallization of zeolites. Pure silica zeolites with a sodalite (SOD) structure were obtained using ethylene glycol as a solvent. Since their study, several types of zeolites like MFI, FER, and MTN have been synthesized using organic solvents.[49,50]

Xu et al.[51] first found that an aluminosilicate dry gel was transformed to MFI in contact with vapors of water, ethylenediame (EDA) and triethylamine (Et_3N) at 453 K. Kim et al.[52] and we[53,54] followed this report, and confirmed that this solid dry-gel conversion technique is useful for synthesizing various types of zeolites. Kim et al. called this method vapor-phase transport (VPT).[52]

In addition, several advantages have been shown to be drawn from the VPT method.[53,54] If the aluminum content would be appropriate, aluminum could be fully incorporated in the zeolitic framework during the early stage of crystallization; crystallization of a Si-rich phase followed. A dry gel can be completely converted to a zeolite by selecting the proper synthetic conditions. This synthetic method offers promising prospects for the synthesis of zeolites possessing the same SiO_2/Al_2O_3 ratio as with that of the parent gel, and the production of zeolites shaped in advance. We therefore expected that the VPT method is prospective for the production of zeolite thin layers on a porous support with a variety of shapes.

Membrane Synthesis. The typical preparation procedure that we have employed for synthesizing zeolitic membranes is as follows. A parent aluminosilicate gel is prepared. Either of two kinds of silica sources, colloidal silica or sodium silicate solution, is used. Anhydrous aluminum sulfate, $Al_2(SO_4)_3$, is used as an alumina source. An aqueous solution of NaOH or H_2SO_4 is added to colloidal silica or sodium silicate solution, respectively, and the resultant silicate gel is mixed with an $Al_2(SO_4)_3$ aqueous solution.

A porous α-alumina support with an average pore diameter of 0.1 μm was used throughout our study. The parent aluminosilicate gel is applied on the support surface by means of conventional dip coating.

After Et_3N, EDA, and water as the vapor source are poured into the bottom of an autoclave, the alumina support coated with the aluminosilicate dry gel is set horizontally in the autoclave, as shown in Fig. 2. The gel is crystallized in the mixed vapors of Et_3N, EDA, and water under autogeneous pressure at 453 K for 4 d.

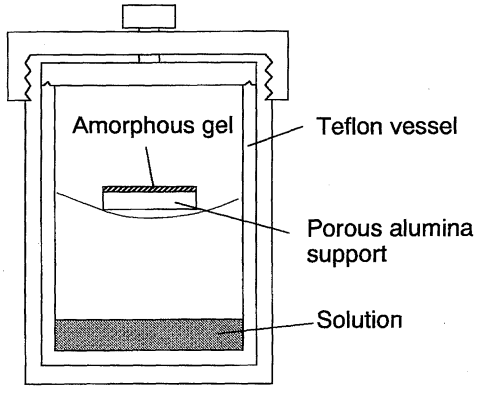

Fig. 2. Schematic diagram of the special autoclave for vapor-phase transport synthesis.

An as-synthesized membrane is calcined in air at 773 K for 4 h. In order to prevent crack formation in the zeolite layer, we employed a heating rate of 0.1 K min^{-1} in the temperature range of 473—773 K.

The formation of a compact dry amorphous gel on the support prior to crystallization is required to form for the preparation of zeolitic membranes in a compact form.[55,56] Numerous cracks were visually observed during the course of drying, even at room temperature when the gel prepared at pH of 11 had been applied to the alumina support. Moreover, the gel which had been prepared at pH of 10 easily scaled off the support during the drying process.

The compactness of the gel can be evaluated by its specific surface area. Figure 3[56] shows the specific surface area of aluminosilicate gel dried at 363 K overnight as a function of the pH at which the gel was prepared. The specific surface areas of both dry gels with SiO_2/Al_2O_3 ratios = 25 and 50 exhibited the same pH dependence, and steeply decreased with increasing pH in the range of 9.5—11.5. This trend indicates that the dry gel becomes compact when the gel is prepared at pH > 11.5.

Further details of the pH dependence were studied using gels prepared at pH of 11.0—12.0. A glass plate was dipped in a gel prepared at a given pH and room temperature. The resultant gel film on the glass plate was dried at 363 K for 1 h. The compactness of the film was visually evaluated, as listed in Table 4.[54] When a sodium silicate solution was used, a compact continuous film with SiO_2/Al_2O_3 ratio = 50 was obtained on a glass plate at pH = 11.66, while numerous cracks were visually observed on a gel film prepared at pH = 11.45. A gel with SiO_2/Al_2O_3 ratio = 25 gave similar results when a sodium silicate solution was used. A value of pH = 12.13 was required for the formation of a continuous compact film when colloidal silica was used. Table 4 also lists the specific surface areas of dry gels. As described above, the specific surface area of either dry gel decreased with increasing pH, indicating that the dry gel became denser at higher pH. In conclusion, it is essential to precisely control the value of the pH for obtaining a compact continuous layer of a dry amorphous gel on the support.

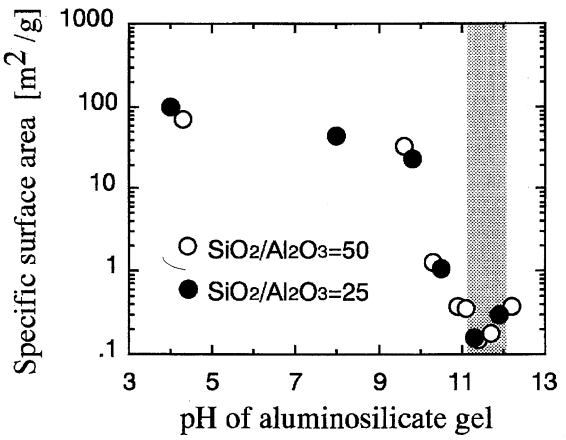

Fig. 3. Effect of pH of at which gel was prepared on its specific area.

Table 4. Effect of pH at Which Gel Was Prepared on the Surface Area and the Compactness of the Dry Gel Film on a Glass Plate

Silica source	SiO_2/Al_2O_3	pH	Specific surface area [M^2 g^{-1}]	Compactness
Sodium silicate Solution	50	11.66	0.21	Good
		11.45	0.27	Poor
	25	11.82	0.20	Good
		11.58	0.43	Poor
		11.28	5.22	Poor
Colloidal silica	25	12.13	0.11	Good
		11.81	0.16	Poor
		11.54	0.20	Poor

$SiO_2/Na_2 = 2.1$.

Elucidating the chemistry of aluminosilicate gel is clearly essential to prepare a nicely compact dry gel layer on a support surface. In general, silicic species exist both in the form of a dissolved state and in solid particles in the synthesis solution. The content of dissolved siliceous species dramatically decreases, and, instead, particles are formed as the pH decreases from 12 to 10.[57] Namely, a larger amount of dissolved silica was transformed into particles during the gelation of a silicic solution at a lower pH. The gel prepared at a higher pH becomes compact, because dissolved siliceous species act as a binder of the particles during drying. A compact gel can thus be prepared using a silica solution containing a sufficient amount of dissolved silica. This discussion suggests that a higher pH value is favorable for preparing a compact gel layer on a support, being in good agreement with our results shown in Fig. 3 and Table 4.

Table 5 summarizes the typical results of crystallization of aluminosilicate gels applied on an alumina support. Aluminosilicate gels were formed at pH = 11.7 and 12.0 from a sodium silicate solution and colloidal silica, respectively, applied to the alumina support, and crystallized at 453 K for 4 d by the VPT method. The results on a Teflon® plate are tabulated together. It should be noted that different products were obtained on the alumina support and the Teflon® plate when the gel with the same composition was applied to both supports. Sodium silicate resulted in analcime (ANA) on the alumina support, while ferrierite (FER) was formed on the Teflon® plate. Colloidal silica gave MOR on the alumina support, while MFI was formed on the Teflon® plate. The

Table 5. Synthesis of Zeolitic Membranes on Porous Alumina Support with and without Surface Treatment

	Silica source	pH	Products
No treatment	Sodium silicate solution	11.7	ANA
	Colloidal silica	12.0	MOR
Surface treatment	Sodium silicate solution	11.7	FER
	Colloidal silica	12.0	MFI
On Teflon® plate	Sodium silicate solution	11.7	FER
	Colloidal silica	12.0	MFI

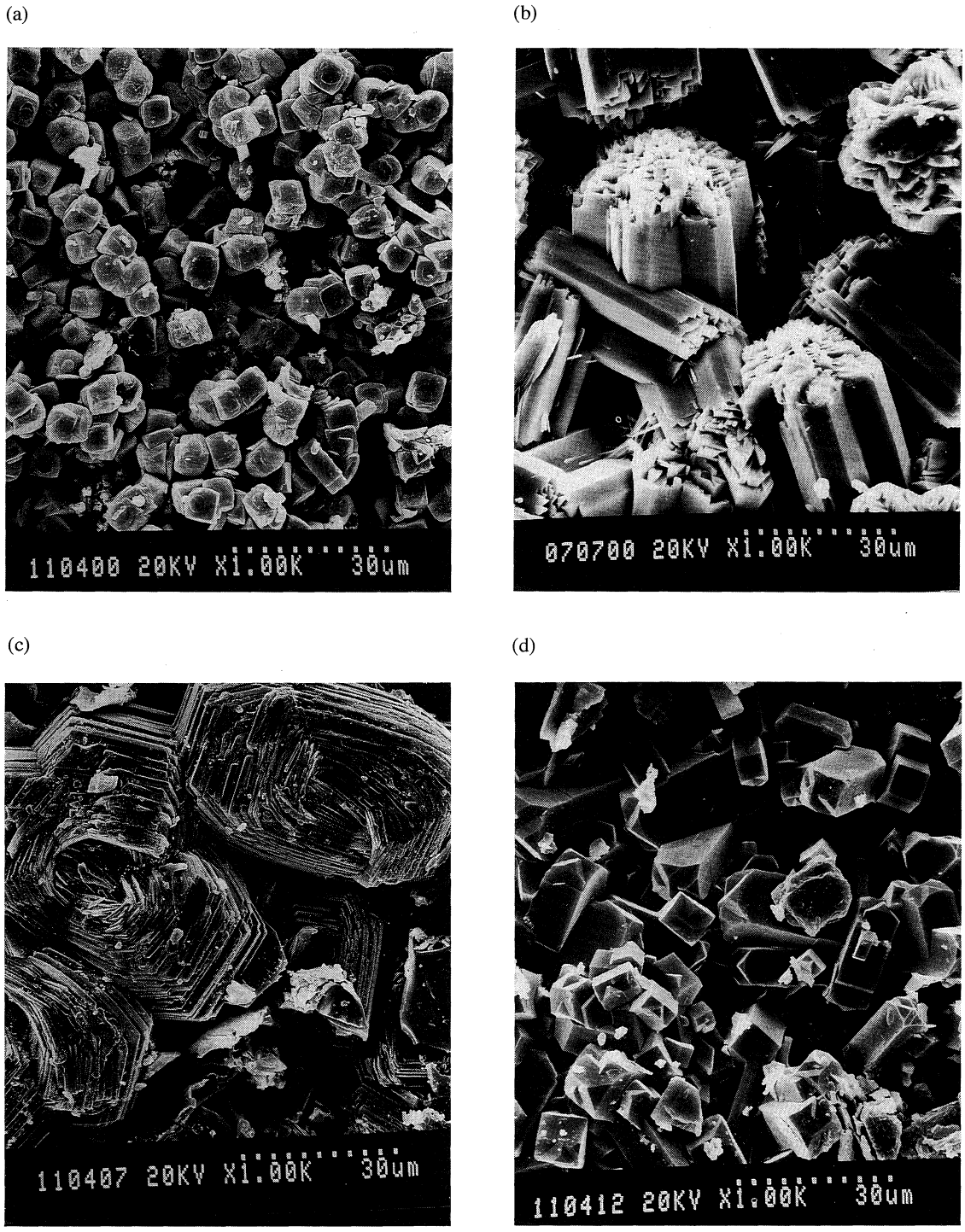

Fig. 4. SEM images for the top views of zeolitic membranes. (a) ANA, (b) MOR, (c) FER, and (d) MFI membranes.

Table 6. Effect of Pore Blocking by Benzene Molecules on Hydrogen Permeation through MOR Membrane

	Permeability of H_2 [mol m^{-2} s^{-1} Pa^{-1}]
Before permeation of benzene	1.12×10^{-7} (310 K)
After permeation of benzene	
Accompanied by evacuation (383 K, 1 h)	2.47×10^{-10} (310 K)
Accompanied by evacuation (400 K, 10 h)	3.48×10^{-8} (310 K)

Permeability of $C_6H_6 = 1.14\times10^{-9}$ (323 K), $\Delta p(C_6H_6) = 0.036$ MPa.

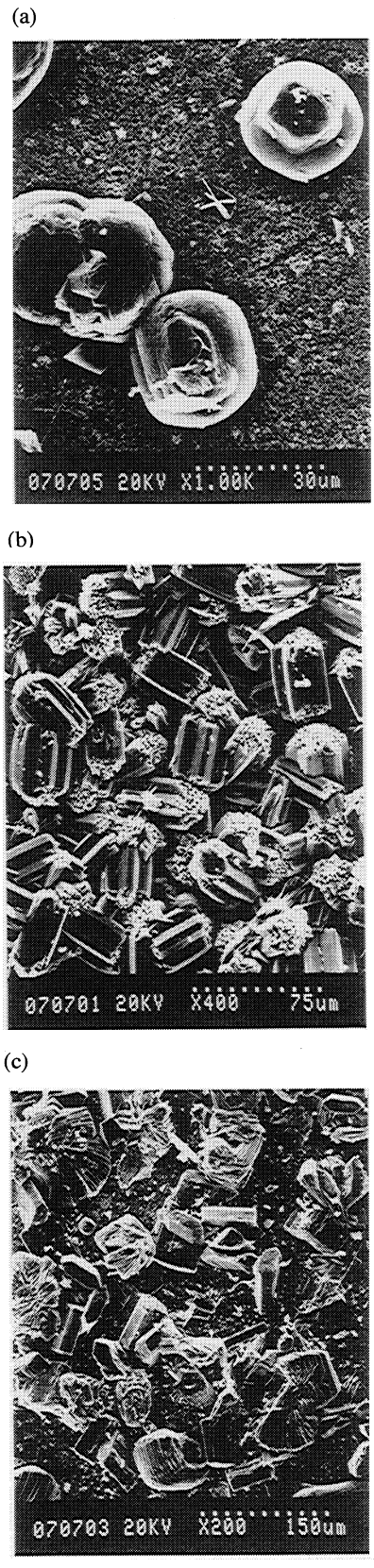

Fig. 5. SEM images for the top views of MOR membranes after (a) 1, (b) 2, and (c) 4 days of crystallization.

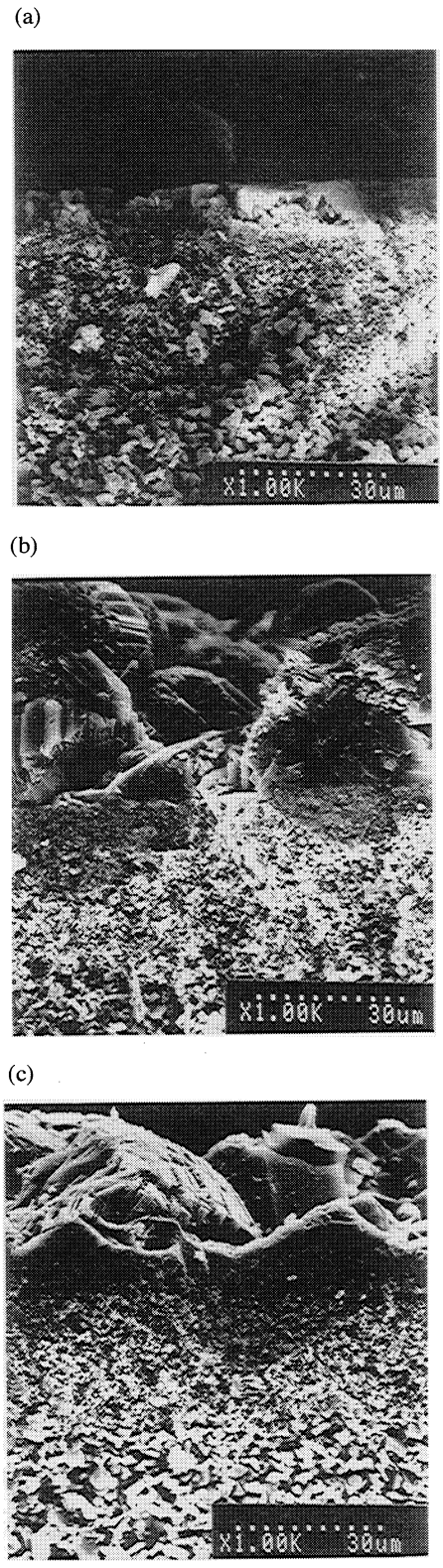

Fig. 6. SEM images for the cross-section of MOR membranes after (a) 1, (b) 2, and (c) 4 days of crystallization.

Fig. 7. FE-SEM images for the cross-section of MOR membrane.

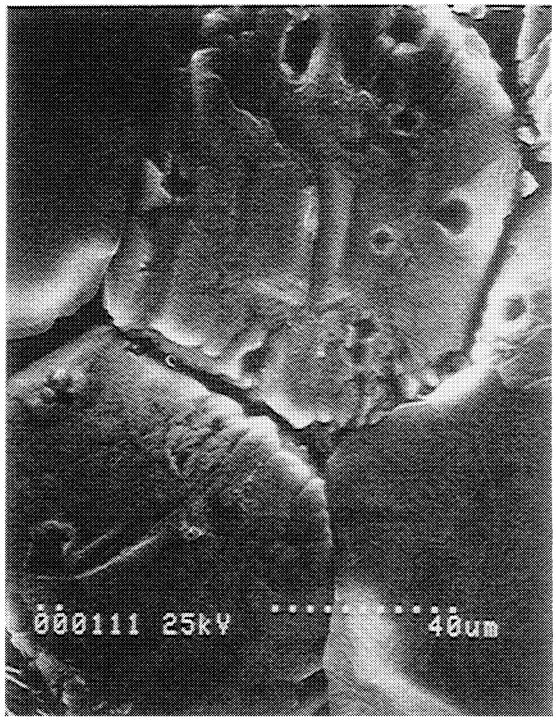

Fig. 9. SEM image for a preferentially oriented MFI membrane prepared on porous alumina support.

SiO_2/Al_2O_3 ratios of ANA and MOR are generally lower than those of FER and MFI: The SiO_2/Al_2O_3 ratios of ANA and FER are typically 4 and 15—20, respectively. Those of MOR and MFI are 8—20 and greater than 20, respectively. These results should be attributed to the dissolution of the alumina support and its incorporation into the framework of zeolite, as found in the studies on hydrothermal synthesis.[25,36]

The surface treatment of the support with colloidal silica, which has a pH of about 10, successfully depressed the dissolution of alumina in our study.[55,56] As can be seen in Table 5, the same crystallization results as those on the Teflon® plate were obtained on the silica-coated alumina support.

Figure 4[56] shows typical SEM images of the top view of the ANA, MOR, FER, and MFI membranes. Each image shows a typical morphology of the corresponding zeolite crystals, the results of which are very different from those observed for those membranes prepared hydrothermally. The top layers of the zeolitic membranes consist of randomly-oriented, isolated crystals. The top views of the zeolitic layers which formed on the surface of the alumina support were clearly incompact.

The pervaporation of 1,3,5-triisopropylbenzene (TIPB), which has a kinetic diameter (0.85 nm) greater than the pore dimensions of FER (0.42×0.54 nm) and MOR (0.65×0.70 nm), was carried out for 10 h at room temperature using the MOR and FER membranes.

No permeation of TIPB through both MOR and FER membranes was detected by gas chromatogram, indicating that the flux of TIPB was less than 1.0×10^{-9} mol m^{-2} s^{-1}, the minimum flux of which can be determined in the experimental procedure used (Table 6). It should be noted that these re-

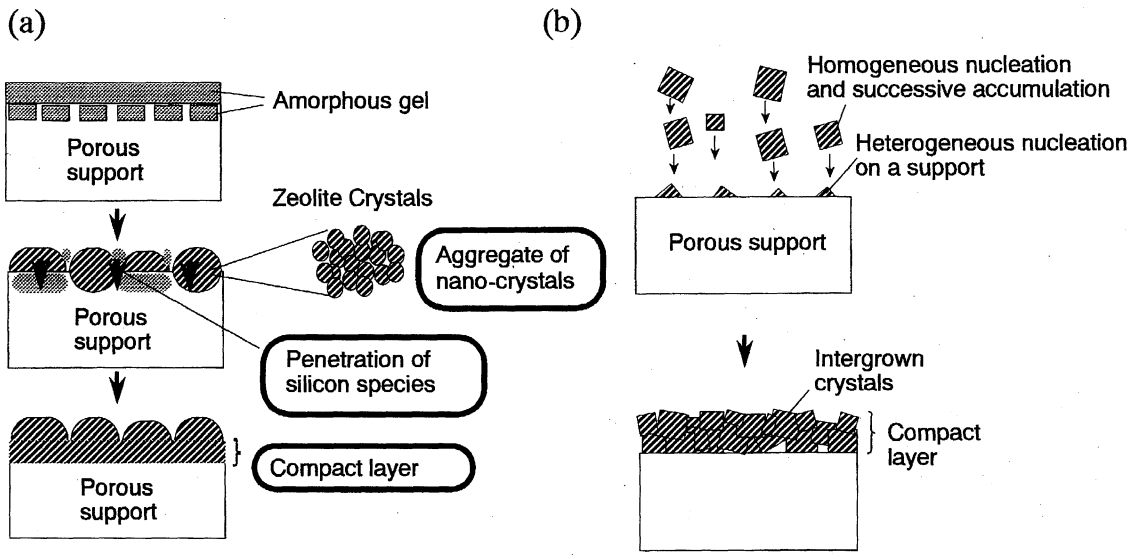

Fig. 8. Formation mechanism of zeolitic membrane (a) by vapor-phase transport method and (b) by hydrothermal synthesis.

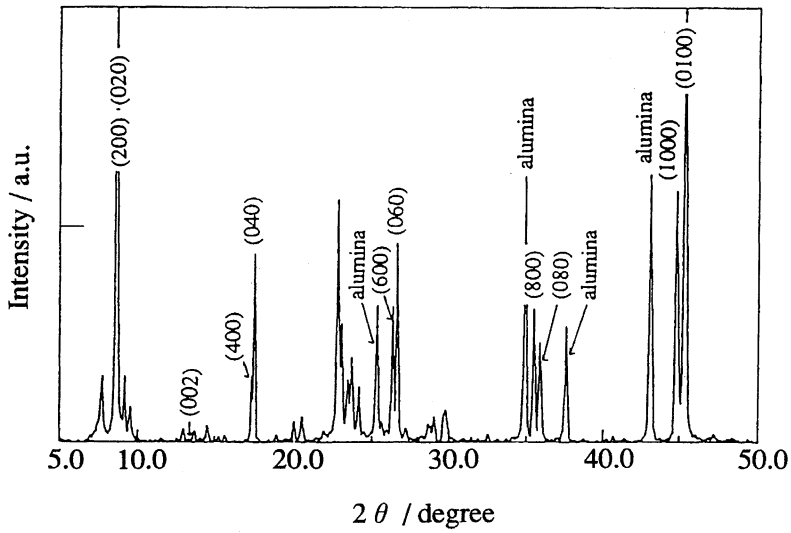

Fig. 10. XRD pattern for a preferentially oriented MFI membrane prepared on porous alumina support.

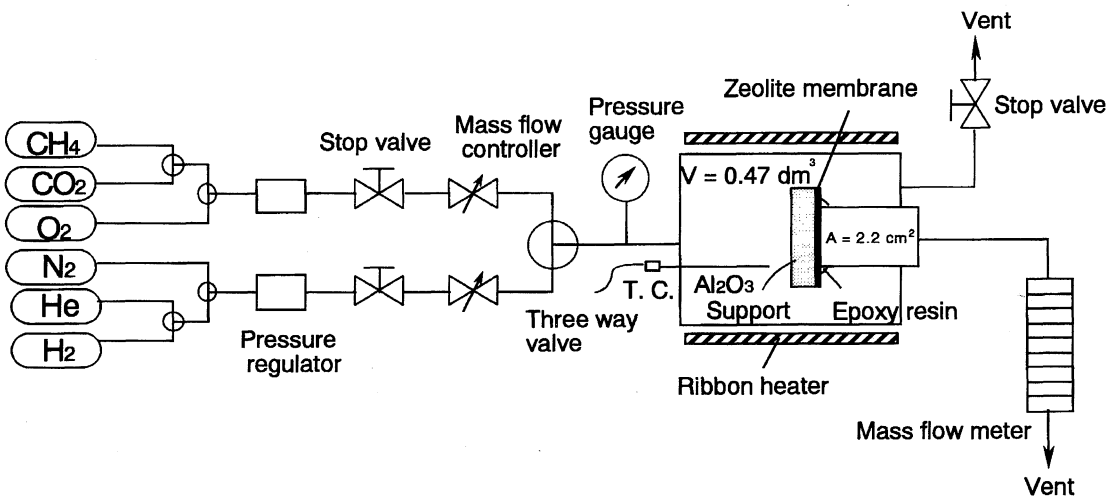

Fig. 11. Schematic diagram of the experimental apparatus for gas permeation measurements.

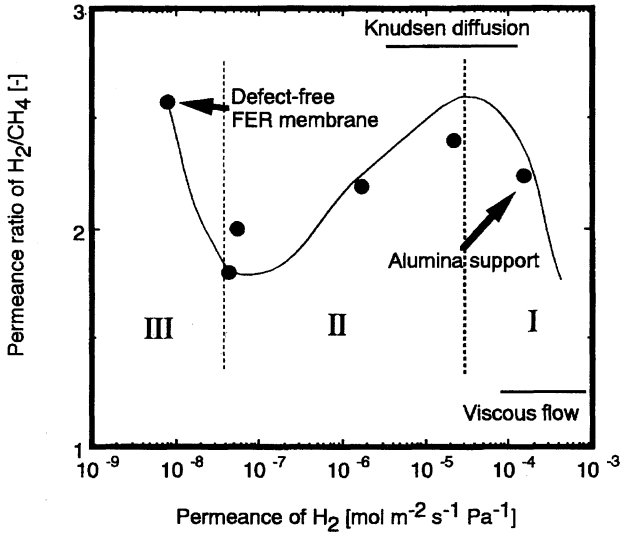

Fig. 12. Permeance ratios of H_2/CH_4 as a function of H_2 permeation through FER membranes. Temperature: 303 K.

sults of permeation tests with TIPB do not necessarily mean that there is no pinhole between the zeolite crystals. We can at least conclude that there practically existed no pinhole greater than the molecular dimension of TIPB in the MOR and FER membranes.

Formation Mechanism of Zeolitic Membranes. It is interesting to note that although numerous voids have been observed among zeolite crystals on an alumina support, as shown in Fig. 4, the MOR and FER membranes are confirmed to be pinhole-free. We have studied the formation mechanism of pinhole-free zeolitic membranes.[55,56,58—60]

We now describe the results of studies on the MOR membrane. Figure 5[56] shows a series of SEM images for the top view of MOR membranes. Figure 5a shows that MOR crystals began to form on the alumina support within 1 d of crystallization. While MOR crystals continued to grow in 2 d (Fig. 5b), the morphology of the MOR crystals was further changed after 4 d (Fig. 5c). Though the MOR membrane was pinhole-free, as previously described, numerous voids were observed among the MOR crystals on the surface of the

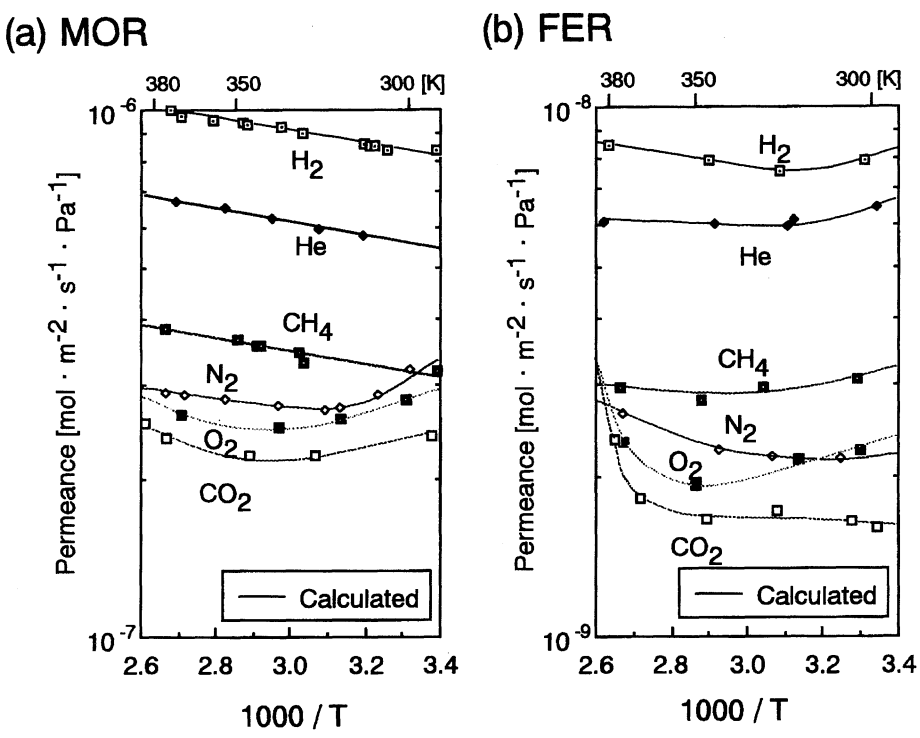

Fig. 13. Permeances of single gases through (a) MOR and (b) FER membranes.

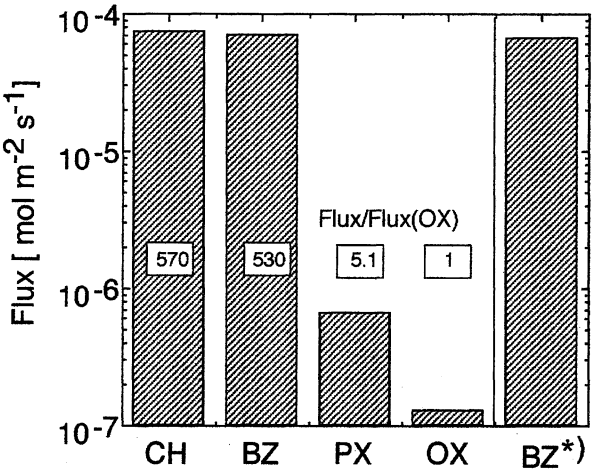

Fig. 14. Pervaporation results for single liquid components using FER membrane. ($T = 303$ K) CH: cyclohexane, BZ: benzene, PX: *p*-xylene, OX: *o*-xylene. *) After permeation test for 1,3,5-triisopropylebenzene.

alumina support. As can be seen from the top views of the MOR layers which formed on the surface of alumina support, the surface of these membranes was clearly not compact.

Figure 6 shows SEM images for the cross-sectional view of the MOR membranes crystallized in different times. It is noteworthy that the part which is bound with MOR crystals formed on the surface of alumina support gave a dark contrast, as shown in Figs. 6a and b. These dark contrast parts spread with the crystallization time, and finally link together after 4 d. Accordingly, these parts seem to be MOR-alumina composite layers.

Judging from Figs. 6b and c, crystallization started at the outer surface, and proceeded to the pores of alumina support to give a continuous MOR-alumina composite layer of 10—20 μm thickness after 4 d. The crystallization mechanism can explain that the MOR-alumina composite layer is pinhole-free, in spite of the fact that there are numerous voids among the MOR crystals on the support.

Figure 7 shows a typical FE-SEM image for the cross section of the MOR membrane. We found that nano-particles fill up the alumina pores. It is believed that these nano-particles are nano-crystals of MOR. Namely, a composite layer consisting of nano-crystals of zeolite and porous alumina can be formed in a compact form. We obtained the same conclusion for the case of an FER membrane.[60,61] During the course of crystallization, Si and Al species can migrate from the outer surface to the interior of alumina pores to fill up the pores.[61] The driving force of such migration might be a concentration gradient, or a capillary force.

Figure 8 schematically illustrates the plausible formation process of zeolitic membranes by the VPT method. Aluminosilicate gel partly penetrates into the pores of the alumina support during the course of dip coating. The crystallization starts on the surface of the alumina support. Then, the crystallization proceeds on both the alumina support and in the pores of alumina. The gel is successively supplied into the pores of the alumina support from the gel layer on the support. The zeolite crystals formed in the pores of alumina support comprize nano-particles. Finally, a zeolite–alumina composite layer is formed in a compact form, while voids remain among the crystals on the alumina support.

The formation mechanisms of zeolitic membranes by hydrothermal synthesis are compared in Fig. 8. Briefly, there are two possibilities for membrane formation, heterogeneous

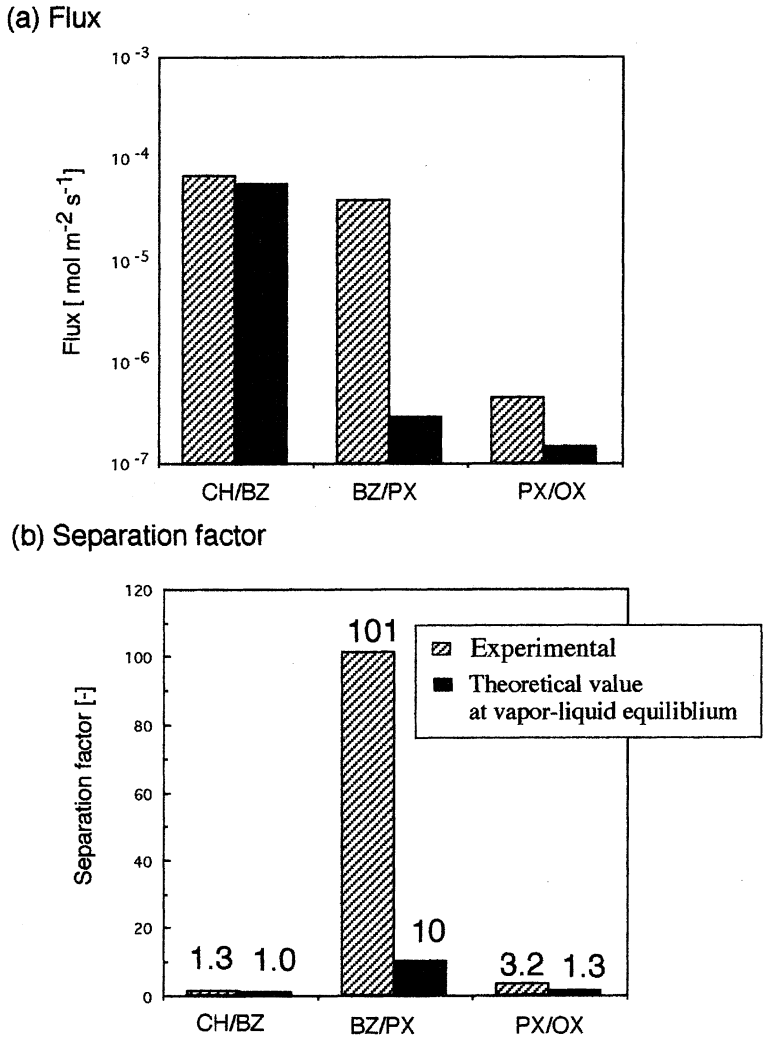

Fig. 15. Pervaporation results for mixtures using FER membrane at 303 K. CH: cyclohexane, BZ: benzene, PX: *p*-xylene, OX: *o*-xylene. Feed mole ratios of CH/BZ, BZ/PX, and PX/OX were 0.95, 1.34, and 0.96, respectively.

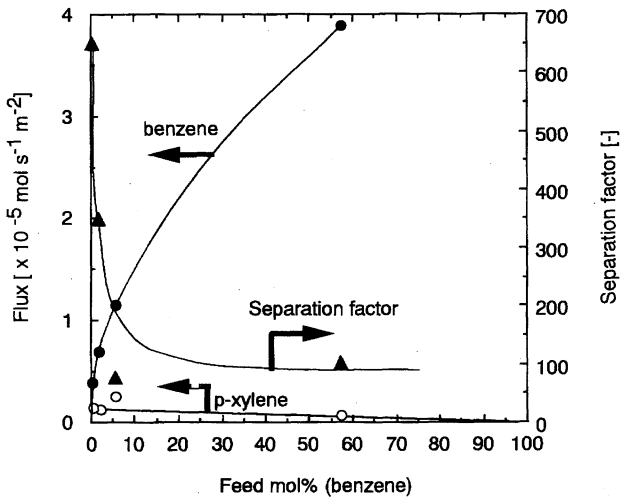

Fig. 16. Effect of benzene feed concentration on the fluxes of benzene and *p*-xylene and separation factor in pervaporation of benzene/*p*-xylene mixtures using FER membranes. Temperature: 303 K, ●: flux of benzene, ○: flux of *p*-xylene, △: separation factor.

and homogeneous nucleation, as discussed above. Irrespective of these mechanisms, once a zeolite layer is formed on the surface of a support, an aluminosilicate solution should find it difficult to penetrate into the support to fill up the pores. Consequently, the intergrowth of crystals formed on the surface of support is probably essential to obtain a pinhole-free zeolitic membrane under hydrothermal conditions, as previously suggested.[22,25,26,33,34,45] The zeolitic membranes prepared by the VPT method, thus, show different morphological features from those prepared by the conventional hydrothermal synthetic method.

Preferentially-Oriented Membrane.[62] Apart from the studies described above, we recently found that preferentially oriented-MFI membrans can be synthesized by the VPT method. The synthesis of pinhole-less, oriented crystals on a porous ceramic support is of great interests for understanding the ultimate permeation properties of zeolitic membranes, and also for sensor and devise applications. Figures 9 and 10 show a typical SEM image and their XRD pattern. These membranes are obtained by using sodium aluminate as an aluminum sourse. Other synthetic procedures are the same as those described above. When aluminum sulfate was used, the MFI layer consisted of an accumulation of randomly ori-

ented polygonal crystals, as shown in Fig. 4. The relative reflection intensities of the (a 0 0) and (0 b 0) crystal faces of MFI are peculiarly high (Fig. 10), indicating that the (a 0 0) and (0 b 0) faces of MFI crystals are oriented pallarel along the surface of the alumina plate. The MFI layer comprizes hexagonal large crystals with a diameter of 50—100 μm; the surfaces of these large crystals are smooth (Fig. 9). It is noteworthy that such an oriented-MFI can be syntheized from a dry gel layer on the support, while the role of the aluminum source involved in the parent gel on the orientation of resultant zeolite crystals is open question.

Permeation Properties of Zeolitic Membranes

Gas Permeation. Although numerous single gas and mixed gas permeation measurements have been reported, the types of zeolitic membranes that have been used for gas-permeation tests are still limited. MFI membranes, especially silicalite (Al-free MFI) membranes, were used frequently. The permeance ratio of *n*-butane to isobutane has been widely used as an indication of the compactness of MFI membranes. However, the relations between the compactness of zeolitic membranes with their permeation and separation properties have not been clearly understood. Compact MFI membranes generally show a high selectivity to *n*-butane, while the selectivity ranges from 1 to 64.[26,27,32—34,63,64]

We carried out permeation tests of H_2 and CH_4 at room temperature with five FER membranes, including a pinhole-free FER membrane and four incompact FER membranes. Figure 11 shows a schematic diagram of the experimental apparatus for determining the permeance of the gas. The pressure difference between the feed and permeate sides was kept at 0.2 MPa. The permeation side was set at atmospheric pressure.

Figure 12 shows the variation in the permeance ratios of H_2/CH_4 plotted as a function of the H_2 permeance through the FER membranes. The H_2 permeance should be an indication of the compactness of FER membranes.

The H_2/CH_4 permeance ratio through the alumina support, itself, was 2.24. The theoretical value for viscous flow and Knudsen diffusion are 1.25 and 2.82, respectively. The H_2/CH_4 permeance ratio through the alumina support is between these two theoretical values. Taking it into account that the average pore diameter of alumina pore is 0.1 μm, this result suggests that the transport of H_2 and CH_4 was governed by the flow in the transition region between viscous flow and Knudsen diffusion. The zeolitic membranes were stuck on a glass or stainless-steel tube with a resin. The effective membrane area was 2.2 cm^2.

The behavior of the H_2/CH_4 permeation ratio can be classified into three regions, as shown in Fig. 12. The H_2/CH_4 permeance ratio approached the theoretical value for the Knudsen diffusion with decreasing H_2 permeance in region I. In region II, the H_2/CH_4 permeance ratio decreased with decreasing H_2 permeance. In this region, the surface diffusion of CH_4, which is more absorbable than H_2, appeared in addition to the Knudsen diffusion. Thus, the H_2/CH_4 permeance ratio is less than the theoretical value for the Knudsen diffusion. In region III, the H_2/CH_4 permeance ratio, again, increases with decreasing H_2 permeance. The extreme left plot in Fig. 12 was obtained with a pinhole-free FER membrane. This behavior seems to be due to configurational diffusion, which influences the permeation of CH_4 more than that of H_2. As a result of this discussion, we suppose that pinhole-free membranes may be essential for separation on the basis of configurational diffusion or shape selectivity. In other words, the smaller number of piholes could greatly influence the permeation and separation properties.

There exists little information on the relation between the separation properties of zeolitic membranes and their structures. We preliminary compared the permeances of inorganic gases through two different types of zeolitic membranes, FER and MOR, synthesized on a porous alumina support.

The permeances of H_2, He, CH_4, N_2, O_2 and CO_2 through these two membranes are shown in Fig. 13.[65] The permeance of each gas through the MOR membrane was about 100-times greater than those through the FER membrane. This was presumably due to the pore diameter of MOR being larger than that of FER, since the thickness of the compact layer in the MOR membrane, about 20 μm, was almost comparable to that of the FER.

The permeances of H_2, He, and CH_4 through the MOR membrane monotonously increased with increasing temperature, indicating that the controlling mechanism of permeation did not change in this temperature region. This temperature dependence of the permeances is evidently caused by activated diffusion. Other permeances of gases through the MOR and FER membranes have minimums with increasing temperature, suggesting that the controlling mechanism changes. The appreance of these minimums can be explained by a combination of activated diffusion and the contribution of sorption. Namely, inorganic gas permeation is governed by an activated diffusion mechanism at higher temperatures, and an increasing amount of gas adsorbed on micropore wall causes an increase in permeance with decreasing temperature. A theoretical analysis of gas permeation through zeolitic membranes was described elsewhere.[65]

Most gas-permeation measurements have so far been carried out below 450 K, except for those described in several reports.[14,32,63,66] This is because it is difficult to seal between a membrane and an apparatus at a high temperature where polymeric sealing materials cannot be used. One of the attractive targets for zeolitic membranes is to develop a highly selective membrane reactor operating at high temperatures. The sealing problems should be overcome in the near future.

Pervaporation Performance. Pervaporation is useful to separate liquid mixtures. Recent studies on separation tests by pervaporation have indicated that zeolitic membranes posses a high separation potential for a variety of organic/water mixtures including water/ethanol[21,48,67] and water/methylethylketone.[68] This separation performance is governed by the hydrophilic/hydrophobic nature of zeolites.

The separation of aromatic hydrocarbons can be achieved by the shape selectivity and/or the adsorption property of zeolites. However, only a few attempts have so far been made

to separate aromatic hydrocarbons. We examined the pervaporation of cyclohexane and three aromatic hydrocarbons, i.e., benzene, *p*-xylene and *o*-xylene, through FER and MOR membranes prepared by the VPT method.[59—61]

Figure 14[61] shows the pervaporation results using the FER membrane for unary systems of cyclohexane, benzene, *p*-xylene and *o*-xylene at 303 K. The zeolitic membrane was set in the solution and the permeate side was kept under a vacuum.

The separation factor ($\alpha(a/b)$) was calculated as follows:

$$\alpha(a/b) = \frac{(x_a/x_b)_{\text{permeate}}}{(x_a/x_b)_{\text{feed}}},$$

where x represents the mole fraction [–].

The ratios of each flux to that of *o*-xylene are shown together in Fig. 14. The fluxes of cyclohexane and benzene are about one-hundred times greater than those of *p*- and *o*-xylene. The flux of *p*-xylene is about five-times greater than that of *o*-xylene.

Pervaporation tests were carried out consecutively in the order from the left to the right-hand side in Fig. 14. The permeation test for TIPB was carried out after that for *o*-xylene, and no permeation of TIPB was detected. After a permeation test for TIPB, pervaporation using benzene was performed again. The flux of benzene observed was comparable to that before the TIPB permeation test, as shown in Fig. 14. These results prove that no TIPB existed in the micropore of FER, and TIPB adsorbed around the entrance of micropores was easily substituted by benzene. This is in good agreement with the conclusion that there existed no pinhole which would allow the entrance of TIPB into the FER membrane.

Figure 15[61] shows the pervaporation results using the FER membrane for binary mixtures, cyclohexane/benzene, benzene/*p*-xylene and *p*-xylene/*o*-xylene at 303 K. The theoretical separation factors from vapor–liquid equilibrium were calculated, and are shown in Fig. 15 together. The separation factors for these three mixtures were greater than those at vapor-liquid equilibrium. It is noteworthy that a separation factor α(*p*-xylene/*o*-xylene) was about 3, taking into account that a MFI membrane which possesses pinholes with a diameter of about 1 nm showed no selectivity for the *p*-xylene/*m*-xylene mixture.[28]

The fluxes of both benzene and *p*-xylene through the FER membrane were about a quarter of those through the MOR membrane. The difference in the fluxes between two types of zeolitic membrane can be attributed to the difference in the pore dimensions of MOR (0.70×0.65 nm) and FER (0.54×0.42 nm). The separation factors for the benzene/*p*-xylene mixture exceeded 100, which was much greater than 10.3 predicted based on the vapor–liquid equilibrium.

The vapor permeation of *p*-xylene, *m*-xylene, ethylbenzene, and toluene through an MFI membrane was carried out by Baertsch et al.,[69] who reported that no separation was achieved for binary mixtures of *p*-xylene/*o*-xylene, *p*-xylene/ethylbenzene, *p*-xylene/toluene, and *m*-xylene/ethylbenzene at 380—480 K. They claimed that the molecule with the slowest permeation rate limits the diffusion, and slows the other species down to its own rate in single-file transport.

When single-file transport occurs in the membrane, the overall selectivity is always governed by the selectivity on the feed side of the membrane. Thus, taking into account that the FER–alumina composite layer is compact, high selectivities for the benzene/*p*-xylene mixtures suggest that the shape selectivity for the benzene/*p*-xylene mixture appears at the pore mouths of FER on the feed side of the FER–alumina composite layer. The intracrystalline diffusivities of benzene in MFI crystals were reported to be comparable to those of *p*-xylene.[70] Therefore, it seems that the difference in the sorption rates of benzene and *p*-xylene molecules into the zeolite pores on the feed side governed the selectivity in the present pervaporation.

Figure 16[60] shows the variation in the fluxes of benzene and *p*-xylene and the separation factor as a function of the feed concentration of benzene. When the molar fraction of benzene in the feed solution was 57 mol%, the separation factors for the benzene/*p*-xylene mixture exceeded 100, which was much greater than 10.3 predicted based on the vapor–liquid equilibrium. The separation factor for benzene/*p*-xylene mixtures greatly increased with decreasing benzene concentration in the feed. The separation factor α (benzene/*p*-xylene) was surprisingly as high as 600 when the feed concentration of benzene was 0.5 mol%. Although the flux of *p*-xylene was varied in proportion to the *p*-xylene concentration in the feed, that of benzene did not monotonously decrease with decreasing feed concentration, suggesting that even when the concentration of benzene in feed solution is extremely small, the sorption rate of benzene into the FER pores still exceeds that of *p*-xylene. Therefore, a high separation factor was obtained at the low feed concentration of benzene.

Concluding Remarks

Only about ten reports on zeolitic membranes were published in 1992. Since then, attention has rapidly been paid to the research on zeolitic membranes and in 1995 more than 150 papers were reported. With this steeply increasing attention, application fields of zeolitic membranes have been expanding, for instance, catalytic membranes, sensors, devices, and modification of electrodes. One can believe that excellent separation properties reported so far prove promising prospects of zeolitic membranes. We have demonstrated that the novel synthetic method, vapor-phase transport, is useful for preparing zeolitic membranes which can be pinhole-free.

On the other hand, the reproducibility is now the most critical problem to be overcome. Most researchers have reported their best results. This is due probably to a lack of knowledge concerning the mechanisms of nucleation and the growth of zeolites. Also, intracrystalline diffusion and sorption properties are still open for discussion. Further fundamental studies in a wide variety of fields of zeolite science are required.

References

1) B. J. Grashoff, C. E. Pilkington, and C. W. Corti, *Platinum Met. Rev.*, **27**, 157 (1983).

2) S. Uemiya, T. Matsuda, and E. Kikuchi, *J. Membr. Sci.*, **56**, 315 (1991).

3) Y. S. Lin and A. J. Burggraaf, *AIChE J.*, **38**, 445 (1992).

4) S. W. Nam and G. R. Gavalas, *AIChE Symp. Ser.*, **85**, 68 (1989).

5) G. R. Gavalas, C. E. Megiris, and S. W. Nam, *Chem. Eng. Sci.*, **44**, 1829 (1989).

6) M. Tsapatsis, S. Kim, S. W. Nam, and G. Gavalas, *Ind. Eng. Chem. Res.*, **30**, 2152 (1991).

7) M. Asaeda, Y. Oki, and T. Manabe, "Priority-Area Research Supported by the Ministry of Education, Science and Culture," Japan, "Energy Conversion and Utilization with High Efficiency," Subarea C (1993), 1993 Research Report, p. 253.

8) A. B. Shelekhin, A. G. Dixon, and Y. H. Ma, *J. Membr. Sci.*, **75**, 233 (1992).

9) M. Bhandarkar, A. B. Shelekhin, A. G. Dixone, and Y. H. Ma, *J. Membr. Sci.*, **75**, 221 (1992).

10) P. Kolsch, D. Venzke, M. Noack, E. Lieske, P. Toussaint, and J. Caro, *Stud. Surf. Sci. Catal.*, **84**, 1075 (1994).

11) M. B. Rao and S. Sircar, *J. Membr. Sci.*, **85**, 253 (1993).

12) M. Niwa, S. Kato, T. Hattori, and Y. Murakami, *J. Chem. Soc., Faraday Trans.*, **80**, 3135 (1984).

13) S. T. Sie, *Stud. Surf. Sci. Catal.*, **84**, 587 (1994).

14) F. Kapteijn, W. J. W. Bakker, J. van de Graaf, G. Zheng, J. Poppe, and J. A. Moulijn, *Catal. Today*, **25**, 213 (1995).

15) H. Suzuki, U.S. Patent 4699892 (1987).

16) L. M. Lachman et al., U.S. Patent 4800187 (1989).

17) Tokkyo Koho, JP 59-213615.

18) Tokkyo Koho, JP 63-287504.

19) T. Sano, Y. Kiyozumi, M. Kawamura, F. Mizukami, H. Takaya, T. Mouri, W. Inaoka, Y. Toida, M. Watanabe, and K. Toyoda, *Zeolites*, **11**, 842 (1991).

20) T. Sano, Y. Kiyozumi, F. Mizukami, H. Takaya, T. Mouri, and M. Watanabe, *Zeolites*, **12**, 131 (1992).

21) T. Sano, F. Mizukami, H. Takaya, T. Mouri, and M. Watanabe, *Bull. Chem. Soc. Jpn.*, **65**, 146 (1992).

22) J. G. Tsikoyiannis and W. O. Haag, *Zeolites*, **12**, 126 (1992).

23) T. Sano, Y. Kiyozumi, K. Maeda, M. Toba, S. Niwa, and F. Mizukami, *J. Mater. Chem.*, **2**, 141 (1992).

24) Y. Kiyozumi, F. Mizukami, K. Maeda, T. Kozasa, M. Toda, and S. Niwa, *Stud. Surf. Sci. Catal.*, in press.

25) E. D. Geus, M. J. Exter, and H. Bekkum, *J. Chem. Soc., Faraday Trans.*, **88**, 3101 (1992).

26) E. D. Geus, H. Bekkum, W. J. W. Bakker, and J. A. Moulijin, *Microporous Mater.*, **1**, 131 (1993).

27) M.-D. Jia, K.-V. Peinemann, and R.-D. Behling, *J. Membr. Sci.*, **82**, 15 (1993).

28) T. Sano, M. Hasegawa, Y. Kawakami, Y. Kiyozumi, H. Yanagishita, D. Kitamoto, and F. Mizukami, *Stud. Surf. Sci. Catal.*, **84**, 1175 (1994).

29) T. Masuda, A. Sato, H. Hara, M. Kouno, and K. Hashimoto, *Appl. Catal., A: General*, **111**, 143 (1994).

30) M. D. Jia, B. Chen, R. D. Noble, and J. L. Falconer, *J. Membr. Sci.*, **90**, 1 (1994).

31) P. Meriaudeau, A. Thangaraj, and C. Naccache, *Microporous Mater.*, **4**, 213 (1995).

32) C. Bai, M.-D. Jia, J. L. Falconer,and R. D. Noble, *J. Membr. Sci.*, **105**, 79 (1995).

33) Y. Yan, M. Tsapatsis, G. R. Gavalas, and M. E. Davis, *J. Chem. Soc., Chem. Commun.*, **1995**, 227.

34) Y. Yan, M. E. Davis, and G. R. Gavalas, *Ind. Eng. Chem. Res.*, **34**, 1652 (1995).

35) Z. A. E. P. Vroon, K. Keizer, M. J. Gilde, H. Verweij, and A. J. Burggraaf, *J. Membr. Sci.*, **113**, 293 (1996).

36) Y. H. Chiou, T. G. Tsai, S. L. Sung, H. C. Shih, C. N. Wu, and K. J. Chao, *J. Chem. Soc., Faraday Trans.*, **92**, 1061 (1996).

37) K. Kusakabe, S. Yoneshige, A. Murata, and S. Morooka, *J. Membr. Sci.*, **116**, 39 (1996).

38) K. Suzuki, Y. Kiyozumi, T. Sekine, K. Obata, Y. Sindo, and S. Sin, *Chem. Express*, **5**, 793 (1990).

39) T. Masuda, H. Hara, M. Kouno, H. Kinoshita, and K. Hashimoto, *Microporous Mater.*, **3**, 565 (1995).

40) H. Mimura, T. Tezuka, and K. Akiba, *J. Nucl. Sci. Technol.*, **32**, 1250 (1995).

41) K. Kita, Horii, Y. Ohtoshi, K. Tanaka, and K. Okamoto, *J. Mater. Sci. Lett.*, **14**, 206 (1995).

42) S. Yamazaki and K. Tsutsumi, *Microporous Mater.*, **4**, 205 (1995).

43) S. Yamazaki and K. Tsutsumi, *Microporous Mater.*, **5**, 245 (1995).

44) G. J. Myatt, P. M. Budd, C. Price, and S. W. Carr, *J. Mater. Chem.*, **2**, 1103 (1992).

45) J. C. Jansen, D. Kashchiev, and A. Erdem-Senatalar, *Stud. Surf. Sci. Catal.*, **85**, 215 (1994).

46) V. Valtchev, S. Mintova, and L. Konstantinov, *Zeolites*, **15**, 679 (1995).

47) M. Tsapatsis, T. Okubo, M. Lovallo, and M. E. Davis, *Mater. Res. Soc. Symp. Proc.*, **371**, 21 (1995).

48) D. M. Bibby and M.P. Dale, *Nature*, **317**, 157 (1985).

49) Q. Huo, S. Feng, and R. Xu, *J. Chem. Soc., Chem. Commun.*, **1988**, 1486.

50) W. Xu, J. Li, W. Li, H. Zhang, and B. Liang, *Zeolites*, **9**, 468 (1989).

51) W. Xu, J. Dong, J. (Jinping) Li, J. (Jianquan) Li, and F. Wu, *J. Chem. Soc., Chem. Commun.*, **1990**, 755.

52) M. H. Kim, H. X. Li, and M. E. Davis, *Microporous Mater.*, **1**, 191 (1993).

53) M. Matsukata, N. Nishiyama, and K. Ueyama, *Microporous Mater.*, **1**, 219 (1993).

54) M. Matsukata, N. Nishiyama, and K. Ueyama, *Microporous Mater.*, **7**, 109 (1996).

55) M. Matsukata, N. Nishiyama, and K. Ueyama, *Stud. Surf. Sci. Catal.*, **84**, 1183 (1994).

56) N. Nishiyama, K. Ueyama, and M. Matsukata, *Microporous Mater.*, **7**, 299 (1996).

57) G. Alexander, "Chemistry in Action Series 1, Silica and Me," Doubleday & Company, Inc., (1967).

58) M. Matsukata, N. Nishiyama, and K. Ueyama, *J. Chem. Soc., Chem. Commun.*, **1994**, 339.

59) N. Nishiyama, K. Ueyama, and M. Matsukata, *J. Chem. Soc., Chem. Commun.*, **1995**, 1967.

60) N. Nishiyama, T. Matsufuji, K. Ueyama, and M. Matsukata, submitted to *Microporus Mater.*

61) N. Nishiyama, K. Ueyama, and M. Matsukata, *Stud. Surf. Sci. Catal.*, **105**, 2195 (1996).

62) E. Kikuchi, K. Yamashita, S. Hiromoto, K. Ueyama, and M. Matsukata, *Microporous Mater.*, in press.

63) W. J. W. Bakker, G. Zheng, F. Kapteijn, M. Makkee, J. A. Moulijn, E. R. Geus, and H. van Bekkum, "Precision Process

Technology," ed by M. P. C. Weijenen and A. A. H. Drinkenburg, Kluwer, Dordrecht (1993), p. 425.

64) W. J. W. Bakker, F. Kapteijn, J. Poppe, and J. A. Moulijn, *J. Membr. Sci.*, **117**, 57 (1996).

65) N. Nishiyama, K. Ueyama, and M. Matsukata, "Proc. 5th World Congr. Chem. Eng.," Vol. 4, p. 834 (1996); submitted to *AIChE J.*

66) R. D. Noble and J. L. Falconer, *Catal. Today*, **25**, 209 (1995).

67) T. Sano, H. Yanagisita, Y. Kiyozumi, F. Mizukami, and K. Haraya, *J. Membr. Sci.*, **95**, 221 (1994).

68) T. Sano, M. Hasegawa, Y. Kawakami, and H. Yanagishita, *J. Membr. Sci.*, **107**, 193 (1995).

69) C. D. Baertsch, H. H. Junke, J. L. Falconer, and R. D. Noble, *J. Phys. Chem.*, **100**, 7676 (1996).

70) D. B. Shah and H. Y. Liou, *Zeolites*, **14**, 541 (1994); D. B. Shah and H. Y. Liou, *Stud. Surf. Sci. Catal.*, **84**, 1347 (1994).

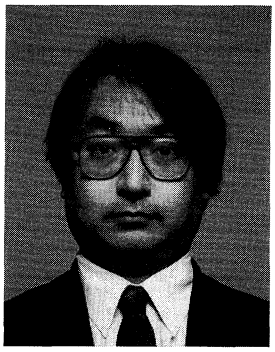

Masahiko Matsukata was born in Tokyo in 1960. He studied applied chemistry at Waseda University and obtained his Dr. Degree in 1989 from the same university under the supervision of Professors Yoshiro Morita and Eiichi Kikuchi. He was appointed research associate of industrial chemistry, Seikei University, in 1989 and then moved to Osaka University as research associate. He was promoted to Associate Professor of Chemical Engineering at Osaka University in 1996 and moved to Department of Applied Chemistry, Waseda University, as Associate Professor in 1997. His research interests range from materials chemistry and engineering, mostly focusing on microporous materials to environmental and energy issues with utilization of fossil fuels.

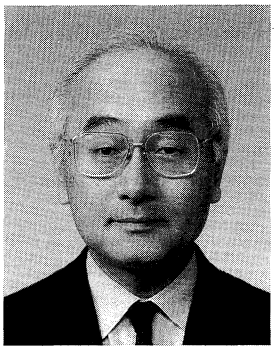

Eiichi Kikuchi was born in Urawa (Saitama) in 1942. He was graduated from the Department of Applied Chemistry, Waseda University in 1964, and received a Ph D from the same university in 1969 on the study of Nickel-catalyzed hydrogenolysis of hydrocarbons. After being a Research Associate (1969—1975) at Waseda University and a Postdoctoral Fellow (1972,73) at the University of Alberta (Canada), he was promoted to Associate Professor in 1975 and Professor in 1980 at Waseda University. Throughout his carrier he was engaged in heterogeneous catalysis, particularly in hydrocarbon conversions, CO hydrogenation, NO reduction, and membrane catalysis.